# Determining the fraction of compact objects in the Universe using supernova observations

Ariel Goobar (Stockholm University)

**Abstract**

This paper examines the use of the gravitational magnification of standard candles, such as Type Ia SNe, to determine the fraction of compact objects in a cosmological context, summarizing the results of Mörtsell, Goobar and Bergström.

The composition of the total energy density is a matter of intense theoretical and experimental research. The density in baryonic matter as derived from Big Bang nucleosynthesis (BBN) is given by $\Omega_{\rm b}h^2 = 0.019 \pm 0.0024$ [1] whereas CMBR measurements yield $\Omega_{\rm b}h^2 = 0.02^{+0.06}_{-0.01}$ [2]. Either way, the baryon density is almost one order of magnitude smaller than the non-baryonic dark matter (DM) component. However, the BBN range for the baryon density still means that most of the baryonic matter is also dark.

There are various possibilities for where the dark baryons hide, e.g. as warm gas in groups and clusters (which is difficult to detect at present [3]), or in the form of massive compact halo objects (MACHOs), where indeed there have been detections [4, 5]. The long lines of sight to distant supernovae mean that they are well suited to probe the matter content along the light paths through gravitational lensing by matter concentrations. Compact objects give lensing effects distinct from diffuse matter. In particular, it may be possible to investigate whether the halo fraction deduced for the Milky Way from microlensing along the line of sight to the Large Magellanic Cloud, of the order of 20 % [4], is a universal number or if the average cosmological fraction is larger or smaller.

Regardless of its constitution, we can classify dark matter according to its clustering properties. In this work we will use the terminology of *smooth DM* for DM candidates which tend to be smooth on subgalaxy scales, e.g., weakly interacting massive particles (WIMPs) such as neutralinos. The term *compact DM* will be reserved for MACHOs such as brown or white dwarfs and primordial black holes (PBHs) [6].

An advantage of gravitational lensing is that its effects can determine the distribution of dark matter independent of its constitution or dynamical state. This paper examines the use of the gravitational magnification of standard candles, such as Type Ia SNe, to determine the fraction of compact objects in a cosmological context, summarizing the results of Mörtsell, Goobar and Bergström [7].

# 1 Compact Objects

An object is compact in a lensing context if it is contained within its own Einstein radius, $r_E$. For a DM clump at $z = 0.5$ and a source at $z = 1$, $r_E \sim 10^{-2}(M/M_\odot)^{1/2}$ pc in a $\Omega_{\rm M} = 0.3, \Omega_\Lambda = 0.7$, $h = 0.65$ cosmology. Also, the Einstein radius projected on the source plane should be larger than the size of the source. A Type Ia SN at maximum luminosity has a size of $\sim 10^{15}$ cm, implying a lower mass limit of $\sim 10^{-4} M_\odot$ for the case described above.

The effects of lensing by compact objects are different from those of lensing by halos consisting of smoothly distributed dark matter, such as in the singular isothermal sphere or Navarro-Frenk-White density profile (NFW; [8]), one of the differences being the probability distribution tail of large magnifications caused by small impact-parameter lines of sight near the compact objects. However, N-body simulations predict, besides the overall cuspy profiles of ordinary Galaxy-sized dark matter halos, also a large number of small subhalos on all length scales which can been resolved [8, 9]. The number density of the smaller objects, of mass $M$, follows approximately the law $dN/dM \propto M^{-2}$ as predicted by Press-Schechter theory [10]. Thus one may expect a multitude of subhalos in each galaxy or cluster halo. In addition, N-body simulations show the less massive halos to be denser (mainly due to them being formed early when the background density was higher). Thus, it is appropriate to address the question whether this type of small-scale structure, and in particular the dense central regions of them, may give rise to lensing effects similar to the ones caused by truly compact objects.

# 2 Gravitational lensing of supernovae

The effect of gravitational lensing on Type Ia SN measurements is to cause a dispersion in the Hubble diagram. Of course, this additional dispersion will be a source of systematic error in cosmological parameter determination with Type Ia supernovae. However, a possible virtue of lensing is that the distribution of luminosities might be used to obtain some information on the matter distribution in the Universe, e.g., to determine the fraction of compact DM in our Universe.

In Fig. 1 we compare the dispersion due to gravitational lensing with the intrinsic dispersion and the typical measurement error for Type Ia SNe. In the upper left panel, we show an ideal Hubble diagram with no dispersion and in the upper right panel we add the dispersion due to lensing (lens) in a universe with 20 % compact objects and 80 % smooth dark matter halos parametrized by the NFW formula [8]. Comparing with the panel in the lower left where the intrinsic dispersion (intr) and measurement error (err) have been included (represented by a Gaussian distribution with $\sigma_m = 0.16$ mag), we see that the effects become comparable at a redshift of unity. In the lower right we see the most realistic simulation with intrinsic dispersion, measurement error and lensing dispersion.

Gravitational lensing effects are calculated by tracing the light between the

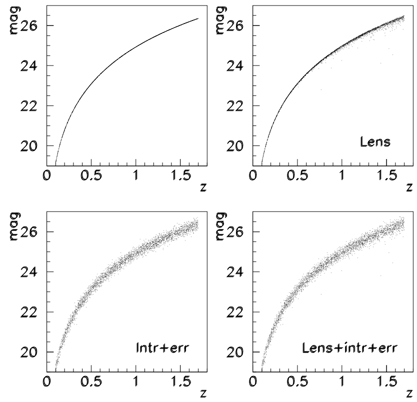


Figure 1: A comparison of the dispersion due to lensing (upper right) and the measurement error and intrinsic dispersion of Type Ia SNe (lower left).

source and the observer by sending it through a series of spherical cells in which the dark matter distribution can be specified. For more details on the method, originally proposed by Holz and Wald, see [11, 12].

We model compact DM as point-masses and smooth DM by the NFW density profile. The exact parameterization of the smooth DM halo profile is not important for the results obtained in this paper and the eventual small-scale structure in the "smooth" component does not act as a compact component [12]. The results are also independent of the individual masses of the compact objects as well as their clustering properties on galaxy scales [11, 12].

To make realistic predictions of the statistics and quality of the supernova sample, we use the projected discovery potential of the Supernova/Acceleration Probe (SNAP) project. Fig. 2 shows the redshift distribution used. (Note that the more recent distribution includes an order of magnitude more SNe at $z > 1.2$.)

# 3 Results

Using SNOC, we have created large data sets of synthetic SNe observations using the following cosmological background parameter values: $\Omega_{\rm M} = 0.3, \Omega_\Lambda = 0.7$, $h = 0.65$ and a variable fraction of compact objects ranging from 0 to 40 %. (For a discussion of how the halo distributions were generated, see [12].) These are used as reference samples.

In Fig. 3 and Fig. 4, we have plotted the dispersion in the reference samples for 0 % (full line), 20 % (dashed line) and 40 % (dotted line) compact objects in logarithmic and linear scale respectively. In the upper panels, the lensing dispersion is plotted, i.e., the dashed line basically corresponds to the scatter

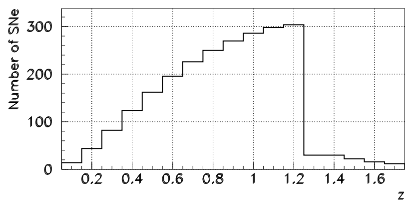


Figure 2: Number of Type Ia SNe expected for various redshift bins in a one-year exposure with the proposed SNAP satellite. The data are taken from Table 7.2 of the Dec. 2000 version of the SNAP science proposal [13]. Note that the more recent SNAP proposal includes an order of magnitude more SNe at $z > 1.2$.

in the upper right panel in Fig. 1. The zero value corresponds to the value one would obtain in a homogeneous universe (upper left panel in Fig. 1). Note that negative values correspond to magnified events, positive values to demagnified events.

As the fraction of compact DM grows, lensing effects becomes larger in the sense that we get a broader distribution of magnifications. From Fig. 3, it is clear how the high magnification tail grows with the fraction in compact objects. In Fig. 4, we see that there is also a shift in the peak of the distribution. In the lower panel we have added a Gaussian intrinsic dispersion and measurement error, $\sigma_{\rm m} = 0.16$ mag, making the distributions look more similar (cf., lower right panel in Fig. 1). Although this smearing obviously decreases the significance of the compact signal, it can be seen that the high-magnification tails and the shifts in the peak of the distributions are still visible.

We have also created a large number of simulated one-year SNAP data sets (according to Fig. 2 above) with 6, 11 and 21 % compact objects. These are our experimental samples. By comparing each generated experimental sample with our high-statistics reference samples using the Kolmogorov-Smirnov (KS) test, we obtain a confidence level for the hypothesis that the experimental sample is drawn from the same distribution as the reference sample. For each fraction of compact objects in the experiments (6, 11 and 21 %), we repeat this procedure for 1000 experimental realizations and pick out the reference sample which gives the highest confidence level for each experiment. Plotting the number of best-fit reference samples as a function of the fraction of compact objects in the reference sample, we can fit a Gaussian and thus estimate the true value and the dispersion. In each case, we get a mean value within 1 % of the true value and a one-sigma error less than 5 %, see Fig. 5.

As one could expect, and is shown in Fig. 1, lensing effects get larger at higher redshifts. At low redshifts the dispersion is completely dominated by the intrinsic dispersion. Therefore, we have only used the data from SNe at $z > 0.8$, a total of 1387 SNe, to obtain the result in Fig. 5.[1]

[1] Of course, the data from SNe at $z < 0.8$ can still be used to constrain the values of $\Omega_{\rm M}$

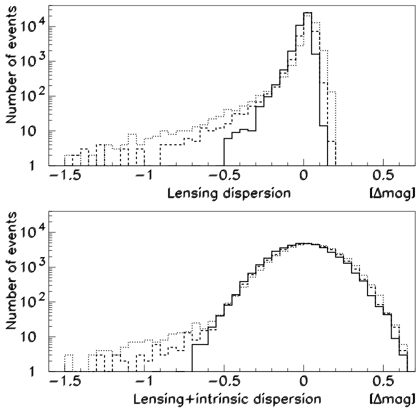


Figure 3: Magnitude dispersion of reference samples for 0 % (full line), 20 % (dashed line) and 40 % (dotted line) compact objects using logarithmic scale. The bottom panel includes a Gaussian smearing, $\sigma_{\rm m} = 0.16$ mag, due to measurement error and intrinsic brightness differences between supernovae. The distributions show the projected scatter around the ideal Hubble diagram for Type Ia supernovae with a relative redshift distribution as in Fig. 2.

Since it is not clear whether the discrimination of samples is most sensitive to changes in the high-magnification tail or to shifts in the peak of the distributions, we have performed a number of statistical tests besides the KS-test, which is most sensitive to differences at the peak of the distributions. These tests includes variants on the KS-test designed to increase the sensitivity in the tails of the distributions (Anderson-Darling, Kuiper, etc.) as well as a maximum likelihood analysis. We have found that the KS-test gives the most robust results for our purposes.

In the analysis so far, we have assumed that $\Omega_{\rm M}$ and $\Omega_\Lambda$ will be known to an accuracy where the error in luminosity is negligible in comparison to the intrinsic and lensing dispersion of Type Ia SNe. This assumption is not unreasonable with future CMBR observations combined with other cosmological tests and the SNAP data itself, nor is it crucial in the sense that we are dealing with the dispersion of luminosities around the true mean value, not the mean value itself. In order to test the sensitivity of our results to changes in the cosmological parameter values, we have performed a number of Monte-Carlo simulations using different sets of parameters in our experimental and reference samples and found the error in the total energy density in compact objects to be negligible[2].

and $\Omega_\Lambda$. In fact, with one year of SNAP data, it is possible to determine $\Omega_{\rm M}$ with a statistical uncertainty of $\Delta\Omega_{\rm M} \approx 0.02$ [13].

[2]Note that the effect from lensing is proportional to the total energy density in compact objects, not the fraction of compact objects, see, e.g., [14]. A higher $\Omega_{\rm M}$ would therefore

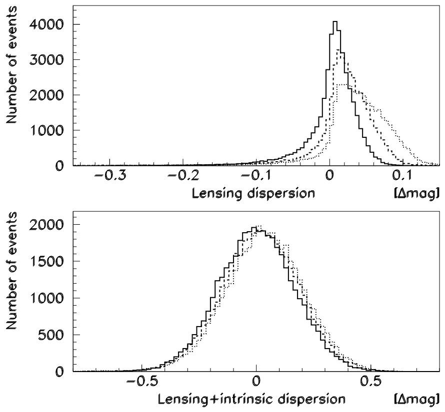


Figure 4: Magnitude dispersion of reference samples for 0 % (full line), 20 % (dashed line) and 40 % (dotted line) compact objects using linear scale (cf., Fig. 3). The bottom panel includes a Gaussian smearing, $\sigma_{\rm m} = 0.16$ mag.

Also, we have used a value of the intrinsic dispersion and measurement error of $\sigma_{\rm m} = 0.16$ mag, a value which may be appreciably smaller in the future when the large data sample expected may allow, e.g., a more refined description and classification of supernovae. Using simulated data sets with $\sigma_{\rm m} = 0.1$ mag, the one-sigma error in the determination of the fraction of compact objects, using the same cosmology as above, becomes less than 3 %, as depicted in Fig. 6.

The virtue of the method we use in this paper is that, since Monte-Carlo methods are used to generate our samples as well as to analyze the data, we do not need to parametrize the probability density functions (pdf's) for different fractions of compact objects. Also, since we use the KS-test, we do not have to bin our data in order to perform our statistical analysis. A possible drawback is that we do not include the effects from large scale structure in our lensing calculations as done in [15]. However, since our modeling of the structure is very detailed up to galaxy scales (see [16]), the two approaches should be complementary to each other. Of course, it should be possible to combine the pdf's from large scale structure with the pdf's from galaxy scales that we obtain from our Monte-Carlo simulations but we have not yet performed such an analysis.

# 4 Summary

The proposed SNAP satellite will be able to detect and obtain spectra for more than 2000 Typa Ia SNe per year. In this paper we have used simulated data sets obtained with the SNOC simulation package to show how one-year SNAP data

increase the sensitivity for smaller fractions.

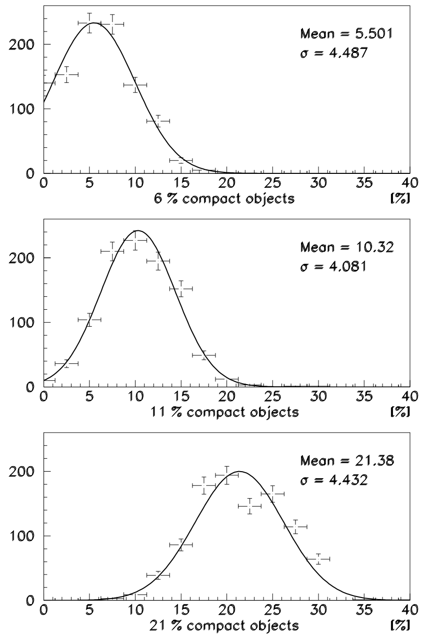


Figure 5: The number of best-fit reference samples as a function of the fraction of compact objects in the reference sample.

can be used to determine the fraction of compact DM in our Universe to $\lesssim 5\%$ accuracy, assuming the intrinsic dispersion and measurement error is $\sigma_{\mathrm{m}} = 0.16$ mag. If the intrinsic dispersion and measurement error can be reduced, e.g., from a better understanding of Type Ia SN detonation mechanisms, the accuracy can be improved even further.

# References

[1] S. Burles *et al.*, Phys. Rev. Lett. 82 (1999) 4176.

[2] X. Wang, M. Tegmark and M. Zaldarriaga, *pre-print* astro-ph/0105091 (2001).

[3] M. Fukugita, C.J. Hogan and P.J.E. Peebles, Astrophys. J. 503 (1998) 518.

[4] C. Alcock *et al.*, Astrophys. J. 542 (2000) 281.

[5] T. Lasserre et al., Astronomy and Astrophys. 355 (2000) 39.

[6] K. Jedamzik, Phys. Rev. D 55 (1998) 5871.

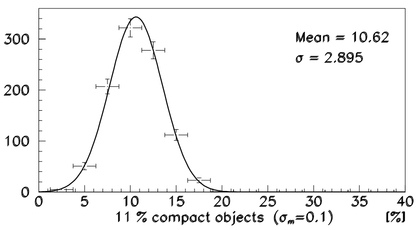


Figure 6: The number of best-fit reference samples as a function of the fraction of compact objects in the reference sample for an intrinsic dispersion and measurement error of $\sigma_{\mathrm{m}} = 0.1$ mag.


[7] E.Mörtsell, A.Goobar and L.Bergström, Astrophys. J, in press (astro-ph/0103489)

[8] J.F. Navarro, C.S. Frenk, and S.D.M. White, Astrophys. J. 490 (1997) 493.

[9] S. Ghigna, B. Moore, F. Governato, G. Lake, T. Quinn and J. Stadel, Astrophys. J. 544 (2000) 616.

[10] W.H. Press and P.L. Schechter, Astrophys. J. 187 (1974), 425.

[11] D.E. Holz, and R.M. Wald, Phys. Rev. D 58 (1998) 063501.

[12] L. Bergström, M. Goliath, A. Goobar, and E. Mörtsell, Astron. Astrophys. 358 (2000) 13.

[13] SNAP Science Proposal, available at `http://snap.lbl.gov` .

[14] P. Schneider, J. Ehlers and E.E. Falco, *Gravitational Lenses* (Springer Verlag, Berlin, 1992).

[15] U. Seljak and D. Holz, Astronom. Astrophys. 351 (1999) L10.

[16] M. Goliath and E. Mörtsell, Physics Letters B 486 (2000) 249.